8. Recombinant fine mapping analysis was performed with single-stranded conformation polymorphisms from the sequence of rescued YAC, BAC, and PAC ends. The YAC ends were rescued by self-circularization, and the BAC/PAC ends were rescued by inverse polymerase chain reaction (PCR) or directly sequenced.
9. Genomic DNA shotgun libraries of BAC14 and PAC14 were made by shearing DNA with a Sonic Dismembrator (20.3 cm by 30.5 cm) (Fisher Scientific) and digesting the DNA with mung bean nuclease. The DNA was then size-selected on agarose gel and blunt-end ligated. High-throughput DNA preps were performed with Qiagene Robot 9600. Shotgun sequencing, estimated to provide fivefold genomic DNA sequence coverage of BAC14 and PAC14, was carried out with an ABI 377 (Perkin Elmer). About 2000 genomic sequences were analyzed with the Phred program. The flanking sequence of the vector was clipped off with CrossMatch. The sequence contigs were assembled with Phrap and edited by Consed.
10. D. Gordon, C. Abajian, P. Green, *Genome Res.* **8**, 195 (1998).
11. C. B. Burge, in *Computational Methods in Molecular Biology*, S. Salzberg, D. Searls, S. Kasif, Eds. (Elsevier, Amsterdam, 1998), p. 127.
12. S. F. Altschul *et al.*, *Nucleic Acids Res.* **25**, 3389 (1997).
13. Filters of a 24 hpf embryonic cDNA library were screened with α^{32}-P–labeled BAC14 or PAC14, which was first annealed in a genomic repeats repressing mixture [5× SSC genomic DNA (2.5 μg/μl), CA and GT oligonucleotide (0.5 μg/μl each), and mermaid repeats (0.5 μg/μl each)] in hybridization buffer [6× SSC, 0.5% SDS, calf thymus DNA (100 μg/μl)] overnight. The filters were then washed in 2× SSC–0.1% SDS, 0.2× SSC–0.1% SDS.
14. P. E. Purdue, J. W. Zhang, M. Skoneczny, P. B. Lazarow, *Nature Genet.* **15**, 381 (1997).
15. C. Leimeister, A. Externbrink, B. Klamat, M. Gessler, *Mech. Dev.* **85**, 173 (1999).
16. O. Nakagawa, M. Nakagawa, J. A. Richardson, E. N. Olson, D. Srivastava, *Dev. Biol.* **216**, 72 (1999).
17. H. Kokubo, Y. Lun, R. L. Johnson, *Biochem. Biophys. Res. Commun.* **260**, 459 (1999).
18. I. Palmeirim, D. Henrique, D. Ish-Horowicz, O. Pourquie, *Cell* **91**, 639 (1997).
19. S. R. Dawson, D. L. Turner, H. Weintraub, S. M. Parkhurst, *Mol. Cell. Biol.* **15**, 6923 (1995).
20. Sense-capped RNA was synthesized for injection with T7 RNA polymerase and the mMESSAGE mMACHINE system (Ambion) after Hind III digestion of *grl* wild type, *grl* mutant with COOH-terminal extension, and *grl* deletion bearing the COOH-terminal truncation. Injection was carried out with a Microinjector 5242 (Eppendorf, Germany).
21. Embryos obtained from grl^{m145} heterozygote incrosses were injected with capped in vitro–transcribed *grl* RNA, of one of three types: wild-type sequence; *grl* mutant sequence (i.e., with COOH-terminal extension); or truncated at amino acid position 250 before the YRPW motif. Various dosages of mRNA were tested. About 55 pg of RNA was used for these experiments. An average of 90% of wild-type embryos injected with 55 pg of grl^{wt}, grl^{mut}, or grl^{del} RNA develop normally. High dosages (about 200 pg) cause more widespread developmental defects in about 60% of embryos.
22. A. L. Fisher, S. Ohsako, M. Caudy, *Mol. Cell. Biol.* **16**, 2670 (1996).
23. For whole-mount RNA in situ hybridization, a 1891-bp fragment of cDNA was subcloned for in vitro transcription. For histological analysis, specimens were fixed in 4% paraformaldehyde, dehydrated, and embedded in plastic (JB-4). Nomarski photomicroscopy was performed with an Axiophot with Ektachrome 160T film (Zeiss). Wild M5 and M10 dissecting microscopes equipped with Nikon cameras were used for low-power photomicroscopy.
24. M. A. Thompson *et al.*, *Dev. Biol.* **197**, 248 (1998).
25. S. Artavanis-Tsakonas, M. D. Rand, R. J. Lake, *Science* **284**, 770 (1999).
26. P. Carmeliet, *Nature* **401**, 657 (1999).
27. W. Liao *et al.*, *Development* **124**, 381 (1997).
28. M. E. Pierpont and J. Moller, in *Genetics of Cardiovascular Disease*, M. E. Pierpont and J. H. Moller, Eds. (Nijhoff, Boston, MA, 1986), p. 13.
29. J. J. Zhang, W. S. Talbot, A. F. Schier, *Cell* **92**, 241 (1998).
30. A. Donovan *et al.*, *Nature* **403**, 776 (2000).
31. We thank X. Kue, S. Sanghvi, S. Childs, M. Yasuda, and C. Simpson for help with DNA sequencing and other technical assistance, and D. Ransom and L. Zon for the *Fli* probe. T.P.Z. is supported by NIH training grant T32HL07208. Supported in part by NIH grants R01RR0888, R01DK55383, and R01HL49579 (M.C.F) and a sponsored research agreement with Genentech (M.C.F.).

11 November 1999; accepted 21 January 2000

DNA Damage–Induced Activation of p53 by the Checkpoint Kinase Chk2

Atsushi Hirao,[1] Young-Yun Kong,[1] Shuhei Matsuoka,[2] Andrew Wakeham,[1] Jürgen Ruland,[1] Hiroki Yoshida,[1]* Dou Liu,[2] Stephen J. Elledge,[2] Tak W. Mak[1]†

Chk2 is a protein kinase that is activated in response to DNA damage and may regulate cell cycle arrest. We generated Chk2-deficient mouse cells by gene targeting. $Chk2^{-/-}$ embryonic stem cells failed to maintain γ-irradiation–induced arrest in the G_2 phase of the cell cycle. $Chk2^{-/-}$ thymocytes were resistant to DNA damage–induced apoptosis. $Chk2^{-/-}$ cells were defective for p53 stabilization and for induction of p53-dependent transcripts such as p21 in response to γ irradiation. Reintroduction of the Chk2 gene restored p53-dependent transcription in response to γ irradiation. Chk2 directly phosphorylated p53 on serine 20, which is known to interfere with Mdm2 binding. This provides a mechanism for increased stability of p53 by prevention of ubiquitination in response to DNA damage.

The maintenance of genomic integrity after DNA damage depends on the coordinated action of the DNA repair system and cell cycle checkpoint controls. The failure of such controls leads to genomic instability and a predisposition to cancer (*1*). Chk2 is a mammalian homolog of the *Saccharomyces cerevisiae* Rad53 and *Schizosaccharomyces pombe* Cds1 checkpoint genes. Chk2 is a protein kinase that acts downstream of ataxia teleangiecstasia mutated (ATM) and may regulate cell cycle arrest (*2–4*).

To investigate the physiological role of Chk2, we generated Chk2-deficient cells by gene targeting in embryonic stem (ES) cells (*5*). The genotype of $Chk2^{-/-}$ ES clones was confirmed by Southern (DNA) blotting (Fig. 1A), and complete loss of Chk2 protein in $Chk2^{-/-}$ cells was confirmed by protein immunoblotting (Fig. 1B) (*6*). Because Chk2 is thought to have a role in the prevention of entry into mitosis (*2–4*), we examined arrest of the cell cycle in ES cells, a cell type in which γ irradiation induces arrest in the G_2 phase but not arrest in the G_1 phase or apoptosis (*7*). Twelve hours after 10 grays (Gy) of γ irradiation, about 90% of both $Chk2^{+/+}$ and $Chk2^{-/-}$ ES cells were arrested with a G_2 DNA content (Fig. 1C). However, at later time points, substantially more $Chk2^{-/-}$ cells entered G_1 and S relative to controls. Examination of only S phase cells marked by a bromodeoxyuridine (BrdU) pulse label gave similar results (Fig. 1C, middle panel). We additionally investigated whether cells were able to enter M phase after γ irradiation by treatment with nocodazole, a microtubule-disrupting agent that traps cells in mitosis (*8*, *9*). In the absence of γ irradiation, about 35% of cells of both genotypes were trapped in mitosis after 12 hours of nocodazole treatment (Fig. 1D). When cells were subjected to γ irradiation with nocodazole treatment, cells of both genotypes arrested in G_2 for 12 hours (Fig. 1D). However, after 18 hours, significantly more $Chk2^{-/-}$ cells entered mitosis. $p53^{-/-}$ ES cells did not show a defect in cell cycle arrest after γ irradiation (Fig. 1C), as previously shown (*7*), indicating that the defect in G_2 arrest observed in $Chk2^{-/-}$ ES cells is p53-independent.

Consistent with these results, asynchronous cells irradiated with 10 Gy showed a reduction in Cdc2-associated H1 kinase activity after 12 hours. However, $Chk2^{-/-}$ cells were unable to maintain this reduction (Fig. 1E). These results indicate that Chk2 is required for the mainte-

[1]The Amgen Institute, Ontario Cancer Institute, and Departments of Medical Biophysics and Immunology, University of Toronto, 620 University Avenue, Suite 706, Toronto, Ontario, M5G 2C1, Canada. [2]Howard Hughes Medical Institute, Verna and Marrs McLean Department of Biochemistry and Molecular Biology, and Department of Molecular and Human Genetics, Baylor College of Medicine, One Baylor Plaza, Houston, TX 77030, USA.

*Present address: Department of Immunology, Medical Institute of Bioregulation, Kyushu University, 3-1-1 Maidashi, Higashi-Ku, Fukuoka 812-8582, Japan.
†To whom correspondence should be addressed. E-mail: tmak@oci.utoronto.ca

nance, but not the initiation, of G_2 arrest induced by DNA damage. Furthermore, they support our previous model, in which Chk2 functions to inhibit Cdc2 activation through inactivation of Cdc25C (*2–4*).

In *S. cerevisiae*, Rad53 controls the transcriptional response to DNA damage, a role played by p53 in mammalian cells (*1*). If Rad53's role is conserved, one might expect Chk2 to function upstream of p53. To test this hypothesis, we evaluated p53-dependent thymocyte apoptosis (*10*). To obtain $Chk2^{-/-}$ thymocytes, we generated somatic chimeras by $Rag1^{-/-}$ blastocyst complementation (*11*). The size and cellularity of thymi of $Chk2^{-/-}$ chimeras ($95 \times 10^6 \pm 6 \times 10^6$ cells) were comparable to those of age-matched 129/J mice ($101 \times 10^6 \pm 9 \times 10^6$ cells) and $Chk2^{+/+}$ chimeras ($105 \times 10^6 \pm 8 \times 10^6$ cells). Flow cytometric analyses of $Chk2^{-/-}$ thymocytes revealed normal development of $CD4^+$ and $CD8^+$ cells (Fig. 2A). Lymph nodes and spleens of $Chk2^{-/-}$ chimeras had normal numbers and ratios of $CD4^+$ and $CD8^+$ $TCR\alpha\beta^+$ T cells (Fig. 2A), indicating that, unlike ATM, Chk2 is not critical for T cell development.

To investigate the role of Chk2 in apoptosis, thymocytes from $Chk2^{+/+}$ and $Chk2^{-/-}$ chimeras and from $p53^{-/-}$ mice were treated with various apoptotic stimuli (*12*). Immature wild-type $CD4^+CD8^+$ thymocytes were highly susceptible to γ irradiation in a dose-dependent manner (Fig. 2, B and C) (*13*). Only 14 and 5% of wild-type thymocytes were viable after 24 and 48 hours of treatment, respectively, with 4 Gy of γ irradiation. In contrast, 68% (24 hours) and 40% (48 hours) of $Chk2^{-/-}$ thymocytes were viable after exposure to the same amount of γ irradiation (Fig. 2C). $Chk2^{-/-}$ thymocytes were also resistant to apoptosis induced by other agents that create double-strand DNA breaks, such as adriamycin (Fig. 2D), but not to apoptotic stimuli that induce single-strand DNA breaks or that activate pathways other than those mediating DNA damage, such as ultraviolet (UV) irradiation, dexamethasone, FasL, or staurosporine (Fig. 2D).

This pattern is similar to that observed in $p53^{-/-}$ thymocytes (*14*, *15*), suggesting that Chk2 may function in the same pathway as p53 during DNA damage–induced apoptosis. To test this, we monitored p53 abundance in γ irradiated $Chk2^{-/-}$ thymocytes. γ irradiation of 5 Gy induced a substantial increase in the amount of p53 protein in $Chk2^{+/+}$ cells, whereas $Chk2^{-/-}$ cells showed no increase (Fig. 3A). Similar results were obtained with activated T cells from $Chk2^{-/-}$ spleens (Fig. 3B) and primary mouse embryonic fibroblasts (MEFs) derived from $Chk2^{-/-}$ ES cells (Fig. 3C) (*16*). Increased amounts of Bax and p21, which are targets for p53 expressed during apoptosis and G_1 arrest, respectively, triggered by DNA damage (*17*, *18*), were observed in wild-type but not $Chk2^{-/-}$ or $p53^{-/-}$ cells exposed to γ irradiation (Fig. 3, A and E). In contrast, UV irradiation resulted in increased amount of p53 in both wild-type and $Chk2^{-/-}$ MEFs (Fig. 3C, right panel), consistent with results obtained for $ATM^{-/-}$ cells (*10*). This result indicates that, like ATM, Chk2 is not required for increased amount of p53 in response to UV irradiation. Furthermore, Chk2 protein was phosphorylated normally in response to γ irradiation in $p53^{-/-}$ cells (Fig. 3A), indicating that phosphorylation of Chk2 does not depend on p53 function.

To confirm that Chk2 regulates expression of p53 after γ irradiation, we introduced the Chk2 gene or a green fluorescent protein (GFP) control construct into $Chk2^{-/-}$ primary MEFs by retroviral transfer (*19*). In the presence of Chk2, increased expression of p53 and p21 in response to γ irradiation was restored (Fig. 3, D and E). These findings indicate that Chk2 acts upstream of p53, regulating the activation of p53 induced by DNA damage.

Phosphorylation of p53 Ser^{15} and Ser^{20} has been detected in response to DNA damage. Ser^{15} is phosphorylated by ATM (*20*, *21*), whereas the kinase for Ser^{20} is unknown. Ser^{20} phosphorylation but not that of Ser^{15} is required to increase the abundance of p53 in response to DNA damage (*22*, *23*). Ser^{20} lies directly on the surface used by Mdm2 to bind p53 and target it for ubiquitination, and phosphorylation of Ser^{20} interferes with Mdm2 binding (*22*). To investigate the mechanism for p53 regulation by Chk2, we performed in vitro kinase assays. Chk2 phosphorylated Ser^{20} on p53, whereas ATM phosphorylated Ser^{15} (Fig. 4, A and B). These results suggest that the increase of abun-

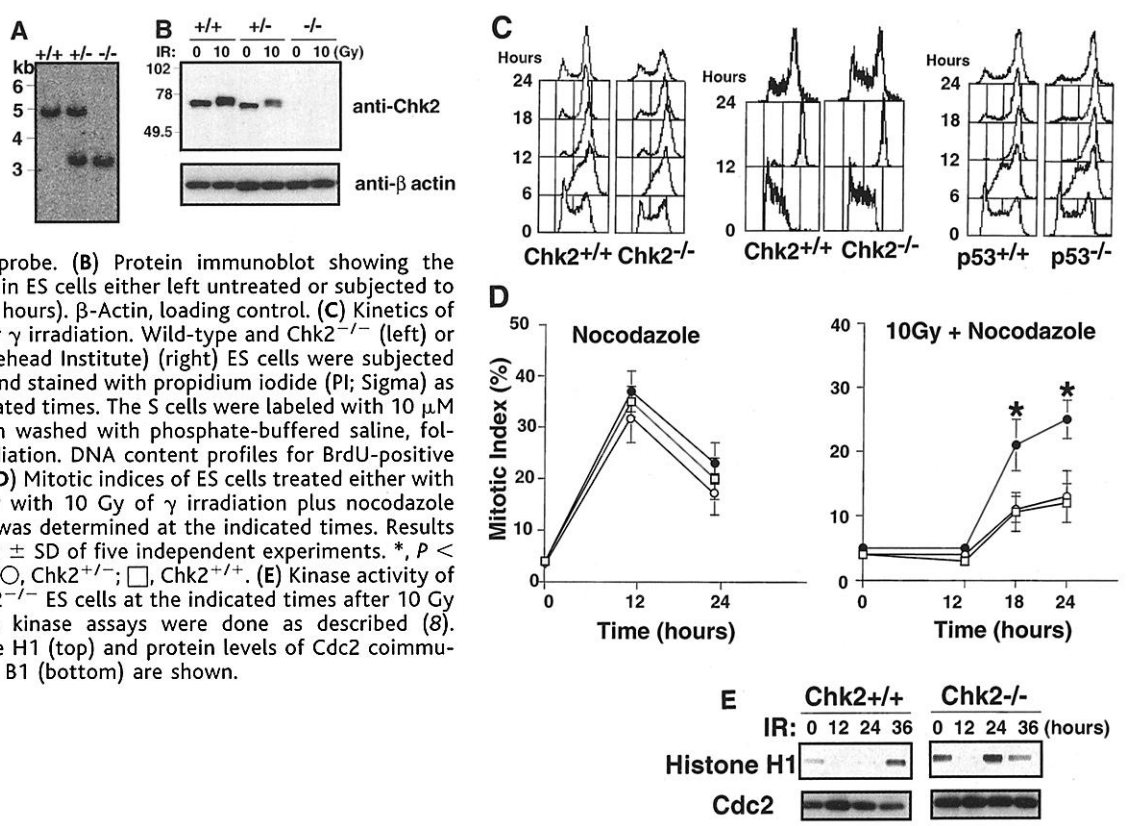

Fig. 1. Failure of maintenance of γ irradiation–induced G_2 arrest in $Chk2^{-/-}$ ES cells. (**A**) Gene targeting of Chk2. Southern blot of Hind III– and Nhe I–digested genomic DNA from $Chk2^{+/+}$(+/+), $Chk2^{+/-}$(+/−), and $Chk2^{-/-}$(−/−) ES cells hybridized to the 5′ flanking probe. (**B**) Protein immunoblot showing the expression of mouse Chk2 in ES cells either left untreated or subjected to γ irradiation (IR) (10 Gy, 3 hours). β-Actin, loading control. (**C**) Kinetics of cell cycle progression after γ irradiation. Wild-type and $Chk2^{-/-}$ (left) or $p53^{-/-}$ (R. Jaenisch, Whitehead Institute) (right) ES cells were subjected to 10 Gy of γ irradiation and stained with propidium iodide (PI; Sigma) as described (*11*) at the indicated times. The S cells were labeled with 10 μM BrdU for 45 min and then washed with phosphate-buffered saline, followed by 10 Gy of γ irradiation. DNA content profiles for BrdU-positive cells are shown (middle). (**D**) Mitotic indices of ES cells treated either with nocodazole alone (left) or with 10 Gy of γ irradiation plus nocodazole (right). The mitotic index was determined at the indicated times. Results shown represent the mean ± SD of five independent experiments. *, $P < 0.01$ (*t* test). ●, $Chk2^{-/-}$; ○, $Chk2^{+/-}$; □, $Chk2^{+/+}$. (**E**) Kinase activity of Cdc2 in $Chk2^{+/+}$ and $Chk2^{-/-}$ ES cells at the indicated times after 10 Gy of γ irradiation. In vitro kinase assays were done as described (*8*). Phosphorylation of histone H1 (top) and protein levels of Cdc2 coimmunoprecipitated with cyclin B1 (bottom) are shown.

dance of p53 after DNA damage is regulated directly by Chk2 phosphorylation in response to ionizing radiation. These results could not be confirmed in vivo because the antibody that recognizes human phosphorylated Ser^{20} does not recognize mouse Ser^{23}, which is the equivalent of human Ser^{20}.

Chk2 has been implicated in checkpoint control through its regulation by ATM and its ability to phosphorylate Cdc25C on an inhibitory residue (*2–4*). In ES cells, we found that Chk2 is required for the maintenance but not for the establishment of G_2 arrest in response to DNA damage. In human colorectal cells or fibroblasts, p53, p21, and 14-3-3sigma have been shown to control maintenance as well (*8*, *24*). However, because p53 loss does not affect G_2 arrest in ES cells, Chk2 is acting in a p53-independent manner to control arrest. This may work through Cdc25C regulation. There must be an additional mechanism to initiate the arrest and that is likely to operate through Chk1, which can also phosphorylate and inhibit the function of Cdc25C (*3*, *25*).

Our results also show that Chk2 activates the key tumor suppressor p53 after DNA damage. Various forms of cellular stress induce marked posttranslational increases in the amount of p53 protein. ATM functions upstream of p53 in vivo (*10*) and can phosphorylate p53 directly in vitro (*20*, *21*). However, it has remained unclear whether ATM alone regulates p53 activation in vivo by direct phosphorylation or whether other molecules are also involved. Our study demonstrates that activation of p53 by DNA damage is impaired in the absence of Chk2 and is consistent with the model shown in Fig. 4C. In response to ionizing radiation, ATM is activated and results in the activation of Chk2. Chk2 can then phosphorylate and inhibit Cdc25C, contributing to maintenance of G_2 for cells in S or G_2, and phosphorylate p53 on Ser^{20}, which prevents Mdm2 binding and results in p53 stabilization. ATM can also phosphorylate p53 on Ser^{15}, which is required for activation of p53 as a transcription factor and may act synergistically with Ser^{20} phosphorylation (*23*). In principle, Ser^{15} phosphorylation could facilitate p53 phosphorylation by Chk2 by a priming-like event. Activated p53 then induces transcription of Bax and other genes to initiate apoptosis in certain cell types and induces p21 to cause inhibition of G_1 Cdks and cell cycle arrest. We were unable to analyze the functionality of the G_1 DNA damage checkpoint in response to γ irradiation because of technical reasons. However, given the defect in p21 induction in $Chk2^{-/-}$ cells, we think it is highly likely that Chk2 mutants will also be defective for this p53-dependent response.

In response to UV damage, neither ATM nor Chk2 are required for activation of p53. How this works is unknown, but we hypothesize it could be through the ATR-Chk1 pathway. Chk1 and Chk2 share substrate specificity to some degree and have been shown to play partially redundant roles in the *S. cerevisiae* DNA damage checkpoint and the *S. pombe* replication checkpoint. Furthermore, we have shown that Chk1 can phosphorylate multiple residues on the NH_2-terminus of p53 (*26*).

Our results indicate that Chk2 is a major effector of the ATM kinase and carries out several of its functions. In addition, because of Chk2's key role in connecting p53 to the response to double-strand breaks, Chk2 is likely to be a tumor suppressor. A recent study identified two heterozygous germ line loss of function mutations in the Chk2 gene in Li-Fraumeni–like syndrome patients without p53 mutation (*27*). Although loss of the wild-type allele of Chk2 in tumors from these patients was not investigated, it is likely that mutant Chk2 is the causative agent in this

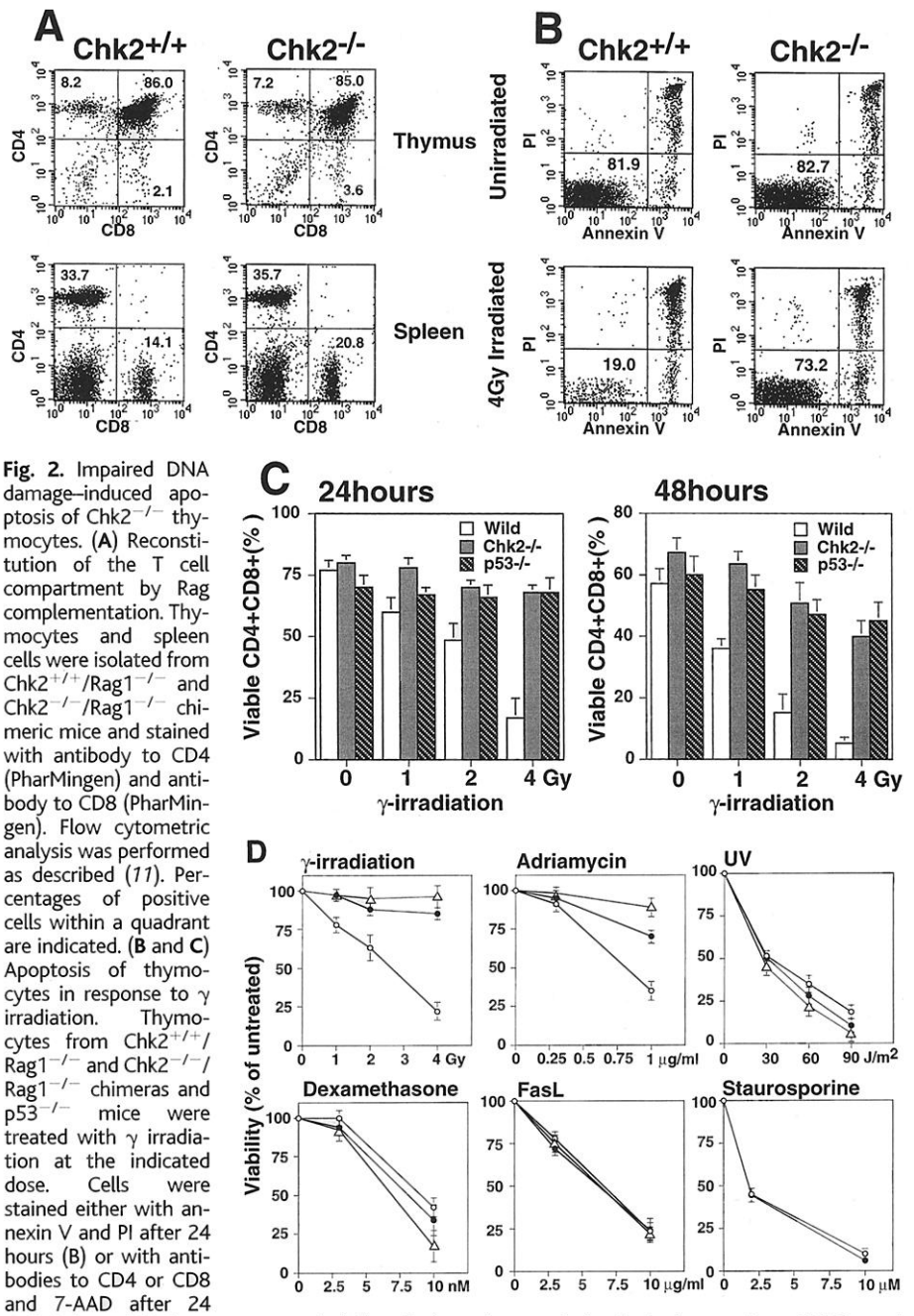

Fig. 2. Impaired DNA damage–induced apoptosis of $Chk2^{-/-}$ thymocytes. (**A**) Reconstitution of the T cell compartment by Rag complementation. Thymocytes and spleen cells were isolated from $Chk2^{+/+}/Rag1^{-/-}$ and $Chk2^{-/-}/Rag1^{-/-}$ chimeric mice and stained with antibody to CD4 (PharMingen) and antibody to CD8 (PharMingen). Flow cytometric analysis was performed as described (*11*). Percentages of positive cells within a quadrant are indicated. (**B** and **C**) Apoptosis of thymocytes in response to γ irradiation. Thymocytes from $Chk2^{+/+}/Rag1^{-/-}$ and $Chk2^{-/-}/Rag1^{-/-}$ chimeras and $p53^{-/-}$ mice were treated with γ irradiation at the indicated dose. Cells were stained either with annexin V and PI after 24 hours (B) or with antibodies to CD4 or CD8 and 7-AAD after 24 and 48 hours (C). The percentage of viable cells (negative population for both annexin and PI) for each sample is shown in (B), whereas the percentage of $CD4^+CD8^+$ cells that remain viable is shown in (C). Open bars, $Chk2^{+/+}$; filled bars, $Chk2^{-/-}$; hatched bars, $p53^{-/-}$. (**D**) Apoptosis of thymocytes treated with various stimuli (*12*), followed by staining with annexin V and PI. Values are normalized to the number of viable cells remaining in untreated cultures derived from the same animal. ○, $Chk2^{+/+}$; ●, $Chk2^{-/-}$; △, $p53^{-/-}$. Data are representative of three independent trials for each experiment. No differences between $Chk2^{+/+}$ chimeras and wild-type littermates of $p53^{-/-}$ mice were observed.

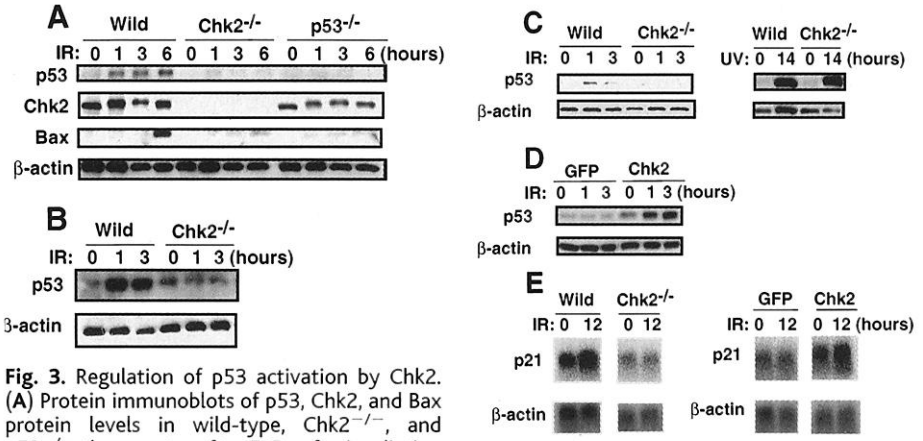

Fig. 3. Regulation of p53 activation by Chk2. (**A**) Protein immunoblots of p53, Chk2, and Bax protein levels in wild-type, $Chk2^{-/-}$, and $p53^{-/-}$ thymocytes after 5 Gy of γ irradiation for the indicated times. Cell lysate proteins were fractionated by SDS–polyacrylamide gel electrophoresis (SDS-PAGE), followed by immunoblotting with antibodies to p53, Chk2, Bax, or β-actin (control). (**B**) Protein immunoblot of p53 in wild-type and $Chk2^{-/-}$ activated T cells after 5 Gy of γ irradiation for the indicated times. Activated spleen T cells (2×10^6/ml) were activated by incubation with concanavalin A (5 μg/ml; Sigma) for 48 hours before irradiation. (**C**) Protein immunoblot of p53 in wild-type and $Chk2^{-/-}$ primary MEFs after 10 Gy of γ irradiation (left) or 60 J/m² of UV irradiation (right) for the indicated times. (**D**) Protein immunoblot of p53 in $Chk2^{-/-}$ primary MEFs infected for 2 days with retrovirus carrying either the Chk2 gene or GFP (control) followed by 10 Gy of γ irradiation for the indicated times. (**E**) Northern blots of wild-type and $Chk2^{-/-}$ primary MEFs (left) and $Chk2^{-/-}$ primary MEFs infected for 2 days with retrovirus carrying either the Chk2 gene or GFP (right), followed by 10 Gy of γ irradiation for the indicated times. Ten micrograms of total RNA isolated by TRIZOL Reagent (Gibco) was transferred to membrane (GeneScreen Plus; NEN Life Science Products) and hybridized with mouse p21 and β-actin cDNAs.

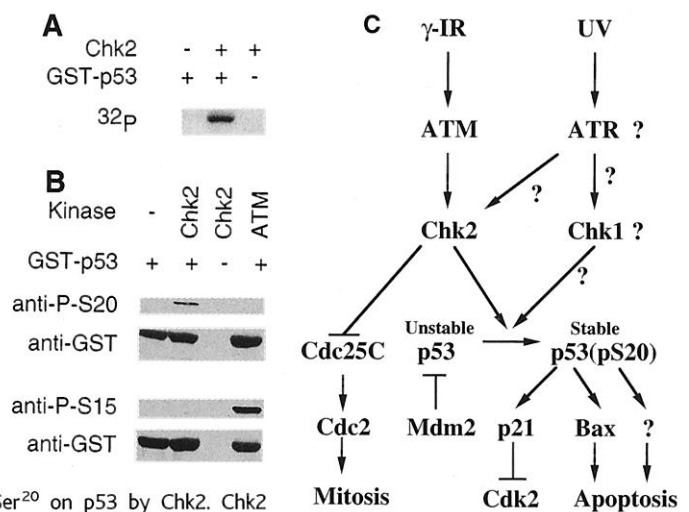

Fig. 4. Chk2 phosphorylates Ser^{20} on p53. (**A**) Phosphorylation of p53 by Chk2. Chk2 was immunoprecipitated from 293T cells with antibody to Chk2 as described (*2*) and then incubated with (+) or without (−) GST-p53(1-80) (*30*) in 50 mM tris-HCl (pH 7.5) and 10 mM $MgCl_2$, 25 μM adenosine triphosphate (ATP), and 10 μCi [γ-^{32}P]ATP for 30 min at 30°C. Proteins were resolved by SDS-PAGE and visualized by autoradiography. (**B**) Phosphorylation of Ser^{20} on p53 by Chk2. Chk2 immunoprecipitated from 293T cells (Chk2) was incubated with (+) or without (−) GST-p53(1-80) in 50 mM tris-HCl (pH 7.5), 10 mM $MgCl_2$, and 25 μM ATP for 30 min at 30°C. FLAG-tagged ATM (ATM) immunoprecipitated with antibody to FLAG from transfected 293T cells was incubated with GST-p53(1-80) as described (*20, 21*). Proteins were resolved by SDS-PAGE and transferred onto nitrocellulose membranes. The membranes were immunoblotted with antibody to phosphorylated Ser^{20} (anti-P-S20) (*31*) or antibody to phosphorylated Ser^{15} (anti-P-S15) (New England Biolab). GST-p53 was visualized by reprobing the membranes with antibodies to GST (anti-GST). (**C**) A model for the role of Chk2 in activation of p53 in response to DNA damage.

cancer predisposition syndrome. Our results provide a mechanistic link between Chk2 and p53 to explain the phenotypic similarity of these two genetically distinct Li-Fraumeni syndrome families. Thus, like p53, Chk2 may contribute to a wide range of human cancers.

References and Notes

1. S. J. Elledge, *Science* **274**, 1664 (1996).
2. S. Matsuoka, M. Huang, S. J. Elledge, *Science* **282**, 1893 (1998).
3. A. Blasina *et al.*, *Curr. Biol.* **9**, 1 (1999).
4. P. Chaturvedi *et al.*, *Oncogene* **18**, 4047 (1999).
5. An 11-kb genomic Chk2 fragment was isolated from a mouse genomic 129/J library. A 5-kb sequence containing exons encoding the kinase domain of Chk2 was replaced by a neomycin cassette inserted in the antisense orientation. E14K ES cells were electroporated with the linearized construct, and G418-resistant ES colonies were identified by polymerase chain reaction and Southern blotting. $Chk2^{-/-}$ ES cell lines were generated by culturing G418-resistant $Chk2^{+/-}$ ES clones in G418 (3.6 mg/ml; Gibco).
6. Protein immunoblots were performed with antibodies to p53 (CM5, Novocastra), mouse Chk2, Bax (Santa Cruz), or β-actin (Sigma), followed by incubation with antibody to rabbit immunoglobulin conjugated to horseradish peroxidase–coupled antibody (Amersham). Proteins were visualized with ECL (Amersham). Rabbit polyclonal antibodies to mouse Chk2 were raised against glutathione S-transferase (GST)–Chk2.
7. P. K. Schmidt-Kastner, K. Jardine, M. Cormier, M. W. McBurney, *Oncogene* **16**, 3003 (1998).
8. F. Bunz *et al.*, *Science* **282**, 1497 (1998).
9. Mitotic indices were determined by the nocodazole trapping method (*8*). ES cells were treated with 10 Gy of γ irradiation, followed by the addition of nocodazole (0.2 μg/ml; Calbiochem). The mitotic index was calculated as the percentage of total cells that were in mitosis.
10. Y. Xu and D. Baltimore, *Genes Dev.* **10**, 2401 (1996).
11. H. Yoshida *et al.*, *Immunity* **8**, 115 (1998).
12. Freshly isolated thymocytes from $Chk2^{+/+}$/$Rag1^{-/-}$ and $Chk2^{-/-}$/$Rag1^{-/-}$ somatic chimeras and $p53^{-/-}$ mice (Jackson Labs) and their control littermates (all 10 to 16 weeks old) were stimulated with γ irradiation (1 to 4 Gy), adriamycin (0.3 to 1.0 μg/ml; Sigma), etoposide (0.1 to 1.0 μM; Sigma), UV irradiation (30 to 90 J/m²; Stratalinker, Stratagene), dexamethasone (3 to 10 nM; Sigma), recombinant CD95-CD8 fusion protein (FasL, 3 to 10 μg/ml), or staurosporine (2 to 10 μM; Calbiochem) for 24 or 48 hours, followed by staining with antibody to CD4-PE, antibody to CD8-fluorescein isothiocyanate (FITC) (PharMingen), and 7-amino-actinomycin D (7-AAD; Sigma) or Annexin V (R&D Systems) plus PI to identify apoptotic cells.
13. K. S. Sellins and J. J. Cohen, *J. Immunol.* **139**, 3199 (1987).
14. S. W. Lowe, E. M. Schmitt, S. W. Smith, B. A. Osborne, T. Jacks, *Nature* **362**, 847 (1993).
15. A. R. Clarke *et al.*, *Nature* **362**, 849 (1993).
16. For generation of primary MEFs, $Chk2^{-/-}$ ES clones and control ES clones ($Chk2^{+/+}$OPGL$^{+/-}$) (*28*) were injected into 3.5-day C57BL/6 blastocysts and transferred to pseudopregnant foster mothers. MEFs were derived from embryonic day 14.5 embryos and selected in G418 (400 μg/ml) for 10 days. Loss of Chk2 protein in $Chk2^{-/-}$ MEFs was confirmed by Western blotting. Cells up to passage 6 were used as primary MEFs.
17. T. Miyashita and J. C. Reed, *Cell* **80**, 293 (1995).
18. J. W. Harper *et al.*, *Cell* **75**, 805 (1993).
19. For retroviral infections, a retrovirus (G. P. Nolan, Stanford University School of Medicine) carrying either the mouse Chk2 or GFP cDNA was packaged with the øNX-Eco cell line, and $Chk2^{-/-}$ MEFs were infected as previously described (*29*). The infection efficiency of GFP was about 60%.
20. S. Banin *et al.*, *Science* **281**, 1674 (1998).
21. C. E. Canman *et al.*, *Science* **281**, 1677 (1998).
22. N. H. Chehab, A. Malikzay, E. S. Stavridi, T. D. Halazonetis, *Proc. Natl. Acad. Sci. U.S.A.* **96**, 13777 (1999).
23. N. Dumaz and D. W. Meek, *EMBO J.* **18**, 7002 (1999).
24. T. A. Chan, H. Hermeking, C. Lengauer, K. W. Kinzler, B. Vogelstein, *Nature* **401**, 616 (1999).
25. Y. Sanchez *et al.*, *Science* **277**, 1497 (1997).
26. Y. Sanchez and S. J. Elledge, unpublished results.
27. D. W. Bell *et al.*, *Science* **286**, 2528 (1999).
28. Y. Y. Kong *et al.*, *Nature* **397**, 315 (1999).
29. Y. Hitoshi *et al.*, *Immunity* **8**, 461 (1998).
30. J. Bargonetti, A. Chicas, D. White, C. Prives, *Cell. Mol. Biol.* **43**, 935 (1997).
31. S. Y. Shieh, Y. Taya, C. Prives, *EMBO J.* **18**, 1815 (1999).

32. We thank the members of the Amgen Institute for helpful discussions; V. Stambolic, L. Harrington, and S. Pownall for critical reading of the manuscript; D. Bouchard for technical support; M. Saunders for scientific editing; G. P. Nolan for retroviral vectors and øNX cells; R. Jaenisch for $p53^{-/-}$ ES cells; K. Tamai and Y. Taya for antibody to phosphorylated Ser^{20} antibodies; and C. Prives for pGST-p53(1-80). Supported by grants from the National Cancer Institute of Canada and Medical Research Council of Canada (T.W.M.) and from the NIH (grant GM44664 to S.J.E.). S.J.E. is an Investigator with the Howard Hughes Medical Institute.

23 November 1999; accepted 18 January 2000